

## Magnetic phase diagram of $\text{Nd}_{1.85}\text{Ce}_{0.15}\text{CuO}_{4+\delta}$ from magnetization and muon spin relaxation measurements

A. Lascialfari,<sup>1,\*</sup> P. Ghigna,<sup>2</sup> and F. Tedoldi<sup>1,†</sup><sup>1</sup>*Department of Physics “A. Volta” and INFM, Via Bassi 6, I-27100 Pavia, Italy*<sup>2</sup>*Department of Physical Chemistry, University of Pavia, Viale Taramelli 16, I-27100 Pavia, Italy*

(Received 27 May 2003; published 25 September 2003)

The magnetic phase diagram of  $\text{Nd}_{1.85}\text{Ce}_{0.15}\text{CuO}_{4+\delta}$  has been investigated up to oxygen content  $\delta \approx 0.064$ . Magnetization, susceptibility, and muon spin relaxation experimental data show that an unconventional spin-glass (SG) phase sets in for  $\delta \geq 0.06$ . A well defined SG-like transition occurs at  $T_g \approx 5$  K for the compound with maximum oxygen content. Below  $T_g$ , however, the shape of susceptibility curves as well as the  $\mu^+$ -polarization recovery laws point out the persistence of residual spin-fluctuations, a signature of a noncomplete freezing of the magnetic lattice. These experimental evidences can be explained by assuming two different slowing down processes for the fluctuations of the Cu and Nd spin ensembles. A phase diagram which agrees with the main results on other high- $T_c$  cuprates is reported.

DOI: 10.1103/PhysRevB.68.104524

PACS number(s): 74.25.Ha, 74.72.Jt, 75.10.Nr, 75.50.Lk

Soon after the discovery of superconductivity in  $\text{Nd}_{2-x}\text{Ce}_x\text{CuO}_4$  (NCCO),<sup>1</sup> this system became one of the reference compounds in the framework of high- $T_c$  superconductors (HTSC's). It exhibits superconductivity for  $0.14 \leq x \leq 0.18$  and has a maximum transition temperature  $T_c \approx 25$  K for  $x = 0.15$ . The prime charge carriers are electrons and for this reason NCCO is clearly distinguished from the hole-doped HTSC's. As in all HTSC cuprates, physical properties are obviously strongly affected by charge carrier density  $\rho$ .<sup>2</sup> The study of the magnetic properties on varying  $\rho$  leads to the determination of a rich phase diagram which is qualitatively similar for all the cuprate HTSC's.<sup>3-9</sup> Starting from the parent antiferromagnetic (AF) compound  $\text{Nd}_2\text{CuO}_4$  ( $\text{La}_2\text{CuO}_4$  for  $\text{La}_{2-x}\text{Sr}_x\text{CuO}_4$ ,  $\text{YBa}_2\text{Cu}_3\text{O}_6$  for  $\text{YBa}_2\text{Cu}_3\text{O}_{6+x}$ ), the magnetic ordering Néel temperature of NCCO diminishes with increasing doping, until  $x \approx 0.14$  where the AF phase disappears and superconductivity sets in.<sup>10</sup> The presence of an intermediate spin-glass (SG) phase, typical of  $\text{La}_{2-x}\text{Sr}_x\text{CuO}_4$  and  $\text{YBa}_2\text{Cu}_3\text{O}_{6+x}$  systems,<sup>3-9</sup> in NCCO has been questioned.<sup>10</sup> In fact, due to substantial difficulties in controlling the doping-carriers content, the details of the HTSC magnetic phase diagram are strongly debated. In NCCO the charge carrier density can be controlled not only by Ce doping but also by varying the oxygen content at fixed Ce stoichiometry. In this paper we will focus on the system  $\text{Nd}_{1.85}\text{Ce}_{0.15}\text{CuO}_{4+\delta}$ .<sup>11,12</sup> By changing the oxygen amount at fixed Ce content, the transport and magnetic properties of this compound are drastically modified.<sup>11</sup> Defining  $n$  the number of electrons per Cu atom ( $n = 0.15 - 2\delta$ ), the system passes from nonsuperconducting to superconducting behavior at  $n = n_0 \approx 0.07$ . No detailed study of the magnetic properties as a function of the oxygen content until the maximum possible amount has been reported and we aim at filling this lack. The resulting magnetic phase diagram is qualitatively similar to all other high- $T_c$  cuprates.<sup>3,5,6</sup>

Powder samples of  $\text{Nd}_{1.85}\text{Ce}_{0.15}\text{CuO}_{4+\delta}$  were prepared as described in Ref. 11, with excess oxygen content  $\delta \approx 0.06, 0.062, 0.064$ . Magnetic susceptibility and magnetization measurements were performed by a MPMS-XL7 Quantum

Design magnetometer, in the temperature range 1.8–300 K at different constant magnetic fields. Hysteresis and relaxation of the magnetization data were collected at  $T = 2$  K on the sample with  $\delta = 0.064$ . The muon spin relaxation ( $\mu^+$ SR) data were collected at the ISIS facility, Rutherford Appleton Laboratory (U.K.), in the temperature range 0.06–300 K in zero and different longitudinal magnetic fields.

For oxygen content  $\delta < 0.045$ ,<sup>11,12</sup> the magnetic susceptibility  $\chi(T)$  data follow the typical behavior of superconducting samples.<sup>12</sup> For  $0.045 < \delta < 0.06$ ,<sup>11,12</sup> the compounds are standard paramagnets mainly due to the contribution of Nd(III) ions to the total magnetization.  $\text{Nd}_{1.85}\text{Ce}_{0.15}\text{CuO}_{4+\delta}$  displays a low-temperature SG-like behavior for  $\delta > 0.06$ . The first evidence comes from the behavior of the zero-field-cooled (ZFC) and field-cooled (FC) susceptibility data, reported in Fig. 1 for the sample with  $\delta = 0.064$  in  $H = 40$  G. As is well known,<sup>13</sup> the maximum in the ZFC data, occurring at  $T \approx 4.5$  K, corresponds to the “spin freezing” temperature  $T_g$  and displaces toward lower temperatures by increasing applied magnetic field (data not reported).

The magnetization hysteresis curve at  $T = 2$  K displayed in the inset of Fig. 2, confirms that the system undergoes a spin-glass transition rather than a transition to a magnetically ordered state, as no hysteretic opening either in FC and ZFC

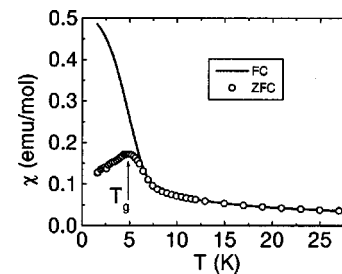


FIG. 1. Magnetic susceptibility  $\chi = M/H$  vs temperature for the  $\text{Nd}_{1.85}\text{Ce}_{0.15}\text{CuO}_{4.064}$  sample in a magnetic field  $H = 40$  G. Both zero-field-cooled (ZFC) and field-cooled (FC) curves are shown. For  $T > 30$  K the experimental data are reproduced by the characteristic paramagnetic behavior  $\chi = C/(T + \theta)$ .

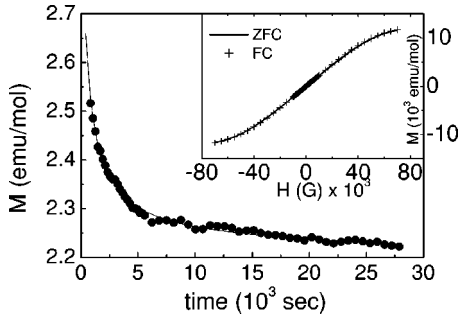


FIG. 2. Relaxation of the magnetization for the  $\text{Nd}_{1.85}\text{Ce}_{0.15}\text{CuO}_{4.064}$  sample, collected at  $T=2$  K (solid circles); the line is a fit of the data according to the model in Eq. (1). In the inset hysteresis data collected either in the ZFC and FC conditions at  $T=2$  K are shown.

conditions is observed. Relaxation data, however (Fig. 2), collected at  $T=2$  K by following the time evolution of the magnetization  $M(t)$  after zero-field cooling of the samples and subsequent application of a magnetic field  $H=7$  T for about 5 min, point out the atypical character of the SG phase. Two different relaxation time-scales are observed in the  $M(t)$  relaxation, so that the attempts to fit the data with “single-exponential-like” functions of the form  $M(t) = M_0 \exp(-\alpha t^{1-d})$ , typical of conventional SG’s,<sup>13</sup> fail. We suggest that at such low temperatures, either Cu and Nd ion spins tend to freeze, giving rise to a complex SG phase. In fact, one obtains a good fit for  $M(t)$  by using a superposition of two SG-like relaxation functions, in the form

$$M(t) = M_0^{\text{Nd}} \exp(-\alpha_{\text{Nd}} t^{1-d}) + M_0^{\text{Cu}} \exp(-\alpha_{\text{Cu}} t^{1-d}), \quad (1)$$

with  $d=0.648$ , close to the value  $d=0.66$  expected in the single-exponential evolution of magnetization in conventional SG formed by a unique type of spins.

To support our hypothesis, we remind what happens in pure and slightly Ce-doped  $\text{Nd}_2\text{CuO}_4$ , which are less disordered systems than the ones considered here. By lowering  $T$ , three different phase transitions to magnetically ordered lattices with different spins rearrangement occur (see, e.g., Ref. 14). At  $T=255$  K, the first phase transition occurs and the Cu spins show a three-dimensional (3D) AF order with a  $\text{La}_2\text{NiO}_4$ -type structure. At  $T=80$  K a second phase transition occurs, and the Cu spins rearrange in a  $\text{La}_2\text{CuO}_4$ -type structure. At  $T=30$  K a third transition is caused by the rearrangement of Cu spins magnetic structure (in  $\text{La}_2\text{NiO}_4$  type again) and, on a second sublattice, by the Nd ions AF order.<sup>14–19</sup> It has to be remarked that at this temperature, Cu and Nd spins sublattices begin to strongly interact. In a way analogous to the  $\text{Nd}_2\text{CuO}_4$  case, in  $\text{Nd}_{1.85}\text{Ce}_{0.15}\text{CuO}_{4+\delta}$ , we expect the complete freezing (often called extreme slowing down) of the Cu spins at higher temperature with respect to the Nd one; this means that, in Eq. (1), one has  $\alpha_{\text{Nd}} > \alpha_{\text{Cu}}$  [from the fit  $\alpha_{\text{Nd}} = (0.175 \pm 0.014)s^{d+1}$  and  $\alpha_{\text{Cu}} = (7.44 \times 10^{-4} \pm 2 \times 10^{-4})s^{d+1}$ ]. We remark that in the parent compound  $\text{Nd}_2\text{CuO}_4$ , the temperature at which Nd spins start to localize is higher with respect to Cu ones. However  $T_{\text{loc}}^{\text{Nd}}$  is indeed very different ( $T_{\text{loc}}^{\text{Nd}} > 70\text{--}100$  K) from the tempera-

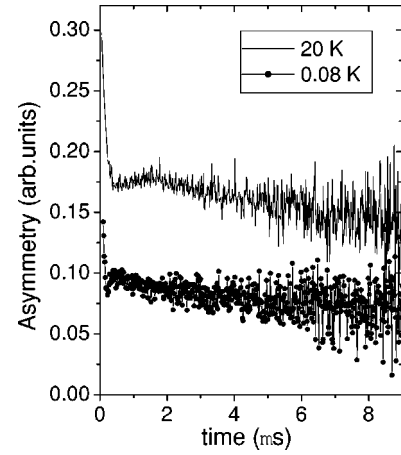


FIG. 3. Muon asymmetry of  $\text{Nd}_{1.85}\text{Ce}_{0.15}\text{CuO}_{4.064}$  at two different temperatures. The data at  $T=20$  K are arbitrarily vertically shifted by 0.1, for the sake of clarity. The presented data correspond to two different temperature regimes (see text).

ture of complete freezing.<sup>14,16</sup> In the experimental data reported in Fig. 1, it is possible to observe the maximum in the ZFC susceptibility at  $T \approx 5$  K that we attribute to the freezing of the Cu spins. The proximity of the two freezing points for Cu and Nd spin ensembles is probably the reason of the sizeable broadening of the maximum in the ZFC curve. The ratio between the local effective magnetic moments at the Nd and Cu sites can be obtained as  $m_{\text{Nd}}/m_{\text{Cu}} = M_0^{\text{Nd}}/M_0^{\text{Cu}} = 1.66/2.29 = 0.72$ , near the value 0.7 found for the magnetically ordered related compound  $\text{Nd}_2\text{CuO}_4$  (data at  $T < 8$  K, Ref. 14). Due to the presence of two different subsets of freezing spins, no scaling argument valid for the spin dynamics in conventional SG (Refs. 7,13) holds and the susceptibility data cannot be fitted by using such scaling arguments.

Further confirmation of the freezing of both sublattices of Nd and Cu spins for  $\delta \geq 0.06$  comes from  $\mu^+$ SR measurements. To study the temperature evolution of the spin dynamics of the two different sublattices, we analyzed the zero-field  $\mu$ SR data on the  $\delta=0.064$  sample. The reader is referred to Ref. 20 for a more detailed examination of  $\mu^+$ SR experiments in longitudinal field and for a comparison between different samples. Here we just recall that the behavior of  $P(t)$  as a function of  $T$  and  $H$  remains qualitatively the same for all the samples with  $\delta \geq 0.06$ . The zero-field data can be analyzed by distinguishing two different temperature regimes: (I)  $4.5 < T < 100$  K, (II)  $T < 4.5$  K (see Fig. 3 for typical raw data in the two regimes). In all the experimental data, the usual background subtraction coming from muons implanted out of the sample, was preliminarily performed. After this subtraction, the muon polarization data can be fitted by a sum of three functions in the range (I) and the sum of two functions in the range (II). Let us now briefly describe the  $P(t)$  fits in the two temperature regions.

(I)  $T > 4.5$  K. In this temperature regime,  $P(t)$  is well reproduced by a sum of two exponential functions plus a Gaussian static Kubo-Toyabe,<sup>21–24</sup> i.e.,

$$P(t) = a_F \exp(-\lambda_F t) + a_S \exp(-\lambda_S t) + f_{\text{KT}}, \quad (2)$$

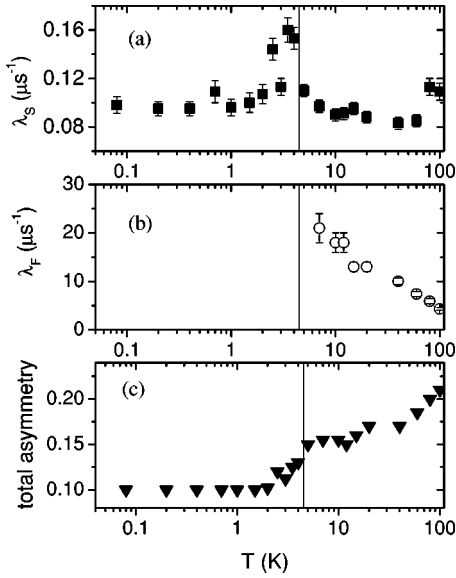


FIG. 4. Temperature behavior ZF- $\mu$ SR spin-lattice relaxation rates of  $\text{Nd}_{1.85}\text{Ce}_{0.15}\text{CuO}_{4.064}$  for muons in site A [ $\lambda_S$  (a)] and in site B [ $\lambda_F$  (b)]; see also text. The solid line marks the transition to the SG-like phase of Cu sublattice. (c) Background subtracted total initial apparent ZF muon asymmetry as a function of temperature. The loss of asymmetry is due to the presence of local fields at the muon sites.

where  $f_{KT} = [1/3 + 2/3(1 - \gamma_\mu^2 \Delta^2 t^2) \exp(-1/2 \gamma_\mu^2 \Delta^2 t^2)]$  ( $\gamma_\mu$  = muon gyromagnetic ratio,  $\Delta$  = second moment of the distribution of local fields at the muon site). In Eq. (2), the relaxation rate  $\lambda_F$  is associated to muons relaxing faster and  $\lambda_S$  to muons relaxing slower.

(II)  $T < 4.5$  K. For  $T < 4.5$  K the exponential component with fast relaxation rate  $\lambda_F$  gives way to a loss of muon asymmetry. The data can be fitted by

$$P(t) = a_S \exp(-\lambda_S t) + f_{KT}. \quad (3)$$

From the above analysis we can conclude that the muons implant in three different sites: (a) site A, muons near the Cu spins, where the muon polarization relaxes fast for  $T > 4.5$  K; (b) site B, muons farther from Cu spins, where the muon polarization relaxes slowly; and (c) site C, near the Nd spins, where  $f_{KT}$  reflects the progressive localization of Nd spins.

The total apparent initial muon asymmetry [Fig. 4(c)] starts to diminish by decreasing  $T$  from 100 K and displays a further clear step at  $T \sim 4.5$  K. We suggest that the loss of muon asymmetry in the range  $4.5 < T < 100$  K is due to muons whose polarization precesses around the local field at the muon site C, created by progressively localizing Nd spins. The low  $T$  ( $< 4.5$  K) loss of asymmetry is associated to the component pertaining to muons in site A, and sets in when the Cu spins slow down to give a SG phase.

We now discuss the spin dynamics as a function of temperature in terms of the evolution of the different fit parameters in Eqs. (2) and (3). The temperature behavior of  $\lambda_F(T)$  shows a divergence by approaching  $T \sim 4.5$  K from above, typical of phase transitions<sup>5</sup> [see Fig. 4(b)]. As said above, below 4.5 K this fast relaxing component disappears [see

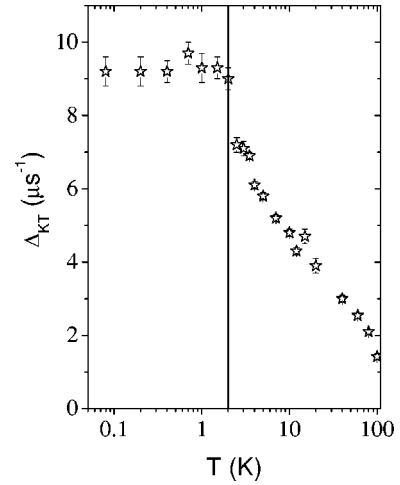


FIG. 5. Temperature behavior of the second moment  $\Delta_{KT}$  of the KT-like component of the total muon asymmetry of  $\text{Nd}_{1.85}\text{Ce}_{0.15}\text{CuO}_{4.064}$ . The low- $T$  flattening corresponds to Nd-spin freezing.

also total asymmetry in Fig. 4(c)] because a local field  $H_{loc}$  at the muon site is present and the precession of the muon polarization around this field occurs at too high frequencies to be detected at the RAL facility ( $H_{loc} > 700$  Oe). Such behavior of  $\lambda_F(T)$  reflects the slowing down of the Cu spin fluctuations when the Cu spins' sublattice approaches the SG transition temperature  $T \sim 4.5$  K. Below 4.5 K, a short-range order of Cu spins is reached, and the related SG-like phase is thought to be similar to the one detected in LASCO and YBCO high- $T_c$  systems for low holes-doping.<sup>5-7,26</sup> It should be remarked that in LASCO and YBCO systems the SG-like phase was evidenced by  $\mu$ SR too.<sup>7,26</sup>

This picture is confirmed by the behavior of  $\lambda_S(T)$  that displays a peak for  $T \sim 4.5$  K [Fig. 4(a)]. This means that muons farther from Cu spins are also sensitive to the slowing-down of the (Cu) spin fluctuations (see, e.g., Ref. 5 for a more extensive treatment of the effect of this slowing-down on a spin-lattice  $T_1$ -like relaxation process).

Let us finally concentrate on the KT-like component. In Fig. 5, the behavior of the second moment of the distribution

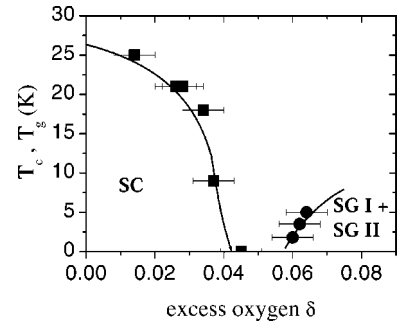


FIG. 6. Magnetic phase diagram of  $\text{Nd}_{1.85}\text{Ce}_{0.15}\text{CuO}_{4+\delta}$ , obtained combining the data of the present work and those of Refs. 11 and 12. For  $\delta \leq 0.045$  the sample is superconducting while for  $\delta \geq 0.06$  a low temperature “exotic” SG-like phase exists with Cu (SGI) and Nd (SGII) spin freezing. For intermediate doping, the magnetic phase character is not yet established.

of local fields  $\Delta(T)$  at the muon site C (i.e., near the Nd ions) is reported. As can be seen, starting from  $T \sim 100$  K,  $\Delta(T)$  tends to increase: at  $T \sim 100$  K its value is  $\sim 1 \mu\text{s}^{-1}$ , while it reaches a plateau  $\Delta(T) \sim 9 \mu\text{s}^{-1}$  for  $T < 2$  K, corresponding to a local fields distribution of width  $\delta H_{\text{loc}} \sim 600$  Oe. This temperature ( $T \sim 2$  K) can be identified as the temperature of extreme slowing down of the Nd spins.

As a final result, the magnetic phase diagram of the compound  $\text{Nd}_{1.85}\text{Ce}_{0.15}\text{CuO}_{4+\delta}$ , deduced after our magnetic susceptibility and  $\mu\text{SR}$  experiments, is reported in Fig. 6. While for  $\delta \leq 0.045$  the system is superconducting, for  $\delta \geq 0.06$  an exotic SG phase sets in. In this phase the Cu and Nd spins tend to order in two spatially disordered magnetic lattices. In Fig. 6 the freezing temperature  $T_g$  of the Cu magnetic mo-

ments is reported (SGI phase), while the characteristic SG transition temperature for the Nd spins (SGII phase) cannot actually be precisely estimated, due to the progressive character of the Nd spin fluctuations slowing down.<sup>25</sup> A very recent paper proved the existence of a strict similarity in the electronic structure between electron (NCCO) and hole (LASCO) doped cuprates.<sup>27</sup> The present paper supports the conclusion that this similarity reflects directly in the magnetic phase diagram.

The authors acknowledge F. Cintolesi and M. Scavini for help with some  $\mu^+\text{SR}$  measurements, and P.J.C. King and J.S. Lord for valuable experimental support.

\*E-mail address: lascialfari@fisicavolta.unipv.it

<sup>†</sup>Present address: Bruker Biospin S.r.l., via Pascoli 70/3, I-20133, Milano, Italy.

<sup>1</sup>Y. Tokura, H. Takagi, and S. Uchida, *Nature (London)* **337**, 345 (1989); H. Takagi, S. Uchida, and Y. Tokura, *Phys. Rev. Lett.* **62**, 1197 (1989).

<sup>2</sup>C.P. Poole, H.A. Farach, and R.J. Creswick, *Superconductivity* (Academic Press, San Diego, 1995).

<sup>3</sup>A. Aharony, R.J. Birgeneau, A. Coniglio, M.A. Kastner, and H.E. Stanley, *Phys. Rev. Lett.* **60**, 1330 (1988).

<sup>4</sup>J.M. Tranquada, A.H. Moudden, A.I. Goldman, P. Zolliker, D.E. Cox, G. Shirane, S.K. Sinha, D. Vaknin, D.C. Johnston, M.S. Alvarez, A.J. Jacobson, J.T. Lewandowski, and J.M. Newsam, *Phys. Rev. B* **38**, 2477 (1988).

<sup>5</sup>A. Rigamonti, F. Borsa, M. Corti, T. Rega, J. Ziolo, and F. Waldner, in *Earlier and Recent Aspects of Superconductivity* (Springer Verlag, Berlin, 1990), p. 441, and references therein.

<sup>6</sup>B. Keimer, N. Belk, R.J. Birgeneau, A. Cassanho, C.Y. Chen, M. Greven, M.A. Kastner, A. Aharony, Y. Endoh, R.W. Erwin, and G. Shirane, *Phys. Rev. B* **46**, 14 034 (1992).

<sup>7</sup>F.C. Chou, F. Borsa, J.H. Cho, D.C. Johnston, A. Lascialfari, D.R. Torgeson, and J. Ziolo, *Phys. Rev. Lett.* **71**, 2323 (1993).

<sup>8</sup>F.C. Chou, N.R. Belk, M.A. Kastner, R.J. Birgeneau, and A. Aharony, *Phys. Rev. Lett.* **75**, 2204 (1995).

<sup>9</sup>A. Campana, R. Cantelli, F. Cordero, M. Corti, and A. Rigamonti, *Int. J. Mod. Phys. B* **14**, 2749 (2000).

<sup>10</sup>G.M. Luke, L.P. Le, B.J. Sternlieb, Y.J. Uemura, J.H. Brewer, R. Kadono, R.F. Kiefl, S.R. Kretziman, T.M. Riseman, C.E. Stronach, M.R. Davis, S. Uchida, H. Takagi, Y. Tokura, Y. Hidaka, T. Murakami, J. Gopalakrishnan, A.W. Sleight, M.A. Subramanian, E.A. Early, J.T. Markert, M.B. Maple, and C.L. Seaman, *Phys. Rev. B* **42**, 7981 (1990).

<sup>11</sup>M. Scavini, P. Ghigna, G. Spinolo, U.A. Tamburini, G. Chiodelli, G. Flor, A. Lascialfari, and S. DeGennaro, *Phys. Rev. B* **58**, 9385 (1998).

<sup>12</sup>A. Lascialfari, P. Ghigna, and S. De Gennaro, *Int. J. Mod. Phys. B* **13**, 1151 (1999).

<sup>13</sup>K. Binder and A.P. Young, *Rev. Mod. Phys.* **58**, 801 (1986).

<sup>14</sup>Y. Endoh, M. Matsuda, K. Yamada, K. Kakurai, Y. Hidaka, G. Shirane, and R.J. Birgeneau, *Phys. Rev. B* **40**, 7023 (1989).

<sup>15</sup>S. Skanthakumar, H. Zhang, T.W. Clinton, W-H. Li, J.W. Lynn, Z. Fisk, and S-W. Cheong, *Physica C* **160**, 124 (1989).

<sup>16</sup>J.T. Markert, E.A. Early, T. Bjornholm, S. Ghamaty, B.W. Lee, J.J. Neumeier, R.D. Price, C.L. Seaman, and M.B. Maple, *Physica C* **158**, 178 (1989).

<sup>17</sup>J.W. Lynn, I.W. Sumarlin, S. Skanthakumar, W-H. Li, R.N. Shelton, J.L. Peng, Z. Fisk, and S-W. Cheong, *Phys. Rev. B* **41**, 2569 (1990).

<sup>18</sup>M. Matsuda, K. Yamada, K. Kakurai, H. Kadowaki, T.R. Thurston, Y. Endoh, Y. Hidaka, R.J. Birgeneau, M.A. Kastner, P.M. Gehring, A.H. Moudden, and G. Shirane, *Phys. Rev. B* **42**, 10 098 (1990).

<sup>19</sup>P. Adelman, R. Ahrens, G. Czjzek, G. Roth, H. Schmidt, and C. Steinleitner, *Phys. Rev. B* **46**, 3619 (1992).

<sup>20</sup>A. Lascialfari, P. Ghigna, F. Cintolesi, M. Scavini, F. Tedoldi, and P.J.C. King (unpublished).

<sup>21</sup>A. Schenck, *Muon Spin Rotation Spectroscopy* (Hilger, Bristol, 1985).

<sup>22</sup>R.S. Hayano, Y.J. Uemura, J. Imazato, N. Nishida, T. Yamazaki, and R. Kubo, *Phys. Rev. B* **20**, 850 (1979).

<sup>23</sup>Y.J. Uemura, T. Yamazaki, D.R. Harshman, M. Senba, and E.J. Ansaldo, *Phys. Rev. B* **31**, 546 (1985).

<sup>24</sup>A. Keren, *Phys. Rev. B* **50**, 10 039 (1994).

<sup>25</sup>For accurate magnetic x-ray scattering investigation of Nd-based cuprates performed at the ESRF facility, Grenoble, see M. D'Astuto (unpublished).

<sup>26</sup>Ch. Niedermayer, C. Bernhard, T. Blasius, A. Golnik, A. Moodenbaugh, and J.I. Budnick, *Phys. Rev. Lett.* **80**, 3843 (1998).

<sup>27</sup>P.G. Steeneken, L.H. Tjeng, G.A. Sawatzky, A. Tanaka, O. Tjernberg, G. Ghiringhelli, N.B. Brookes, A.A. Nugroho, and A.A. Menovsky, *Phys. Rev. Lett.* (to be published).